Limnol. Oceanogr., 56(6), 2011, 2391–2401

doi:10.4319/lo.2011.56.6.2391

Distinct bacterial groups contribute to carbon cycling during a naturally iron fertilized phytoplankton bloom in the Southern Ocean

Ingrid Obernosterer,[a,b,*] Philippe Catala,[a,b] Philippe Lebaron,[a,b,c] and Nyree J. West[a,c]

[a] Université Pierre et Marie Curie, UMR 7621, Laboratoire d'Océanographie Microbienne, UMS 2348, Observatoire Océanologique, Banyuls sur Mer, France

[b] Centre Nationale de la Recherche Scientifique, UMR 7621, Laboratoire d'Océanographie Microbienne, Observatoire Océanologique, Banyuls sur Mer, France

[c] Centre Nationale de la Recherche Scientifique, UMS 2348, Observatoire Océanologique, Banyuls sur Mer, France

Abstract

We investigated the contribution of distinct bacterial groups to bulk abundance and leucine incorporation during a spring phytoplankton bloom induced by natural iron fertilization in the Southern Ocean (Kerguelen Ocean and Plateau Compared Study, January–February 2005). Oligonucleotide probes were designed to target five operational taxonomic units (OTUs) at a narrow phylogenetic level (≥ 99% identity of the 16S ribosomal ribonucleic acid [rRNA] gene). During the peak of the phytoplankton bloom, the *Roseobacter* groups NAC11-7 and RCA, the OTUs SAR92 belonging to Gammaproteobacteria, and the Bacteroidetes OTU Agg58 dominated bulk abundance and leucine incorporation. These four OTUs disappeared with the decline of the bloom, when the cosmopolitan groups SAR11 and SAR86 became dominant. In high-nutrient, low-chlorophyll waters and at a site characterized by transient high phytoplankton biomass, the SAR11 and SAR86 clusters and a *Polaribacter* OTU dominated abundance and leucine incorporation in the upper 100 m. Our results demonstrate that a few distinct bacterial groups identified on a relatively narrow phylogenetic level account for 47% to 82% of bulk abundance and leucine incorporation during the spring phytoplankton bloom in the naturally fertilized region off Kerguelen. The major role of these bacterial groups in carbon cycling in response to natural iron fertilization in the Southern Ocean suggests they could play an important role in the coupling of the biogeochemical cycles of carbon and iron.

Biogeochemical processes in the Southern Ocean are key for the global ocean and atmosphere. Due to the continuous supply of high concentrations of major inorganic nutrients, surface waters of the Southern Ocean hold a large potential for biological activity, in particular primary production and carbon dioxide drawdown. Biological processes are, however, limited by the essential nutrient iron. Several mesoscale fertilization experiments (reviewed in Boyd et al. 2007) and two investigations in naturally fertilized environments (Blain et al. 2007; Pollard et al. 2009) were undertaken to better understand the biogeochemical consequences of iron addition to the Southern Ocean. Independent of the mode of iron fertilization, all these studies have clearly demonstrated that the addition of iron to Southern Ocean surface waters stimulates phytoplankton primary production. In contrast, the response of the heterotrophic microbial community and of higher trophic levels to the phytoplankton bloom induced by iron fertilization varied significantly between studies (Arrieta et al. 2004; Zubkov et al. 2007). As a consequence, the question of how iron addition effects carbon cycling and finally carbon sequestration is far from being resolved.

Two of the major new sources of iron to the Southern Ocean are atmospheric aerosols and lithogenic iron (Jickells et al. 2005). The supply of lithogenic iron is of particular importance in island wakes, and physical processes such as currents, internal tides, and the vertical diffusive flux determine iron concentrations in surface waters. Elevated concentrations of phytoplankton biomass during spring in waters surrounding islands are frequent phenomena and they were suggested to be due to this mode of fertilization (Blain et al. 2001). However, only recently comprehensive studies were carried out in the wake of the Kerguelen (Blain et al. 2007) and Crozet Islands (Pollard et al. 2009) to investigate the effect of natural fertilization on ecosystem structure and ocean biogeochemistry.

The Kerguelen Ocean and Plateau Compared Study (KEOPS) clearly demonstrated that the annually occurring spring phytoplankton bloom southeast of Kerguelen Island is driven by the continuous supply of dissolved iron and also major nutrients from deep waters to the surface (Blain et al. 2007). Microphytoplankton were the most important contributors to the Kerguelen bloom, with an evolution of the dominant phytoplankton groups from the *Chaetoceros* subgenus *Hyalochaete* to *Eucampia antarctica* from the peak to the decline of the bloom, respectively (Armand et al. 2008). Heterotrophic bacteria (Bacteria and Archaea) revealed a marked response to this phytoplankton bloom in terms of bulk abundance, leucine incorporation, and respiration, a finding that clearly contrasts observations from mesoscale fertilization experiments (for references *see* Obernosterer et al. 2008). During the Kerguelen bloom, heterotrophic bacteria processed roughly 45% of gross primary production. These observations raise the question on the composition of the bacterial community that drives carbon processing, and its potential implications on the cycling of both carbon and iron.

The bacterial community associated with the Kerguelen bloom revealed distinct differences as compared to high-

* Corresponding author: ingrid.obernosterer@obs-banyuls.fr

Table 1. Environmental parameters at the study sites. MLD, wind mixed-layer depth.

Sta.	Date	MLD (m)*	Temperature MLD (°C)	$NO_3^- + NO_2^-$ (μmol L^{-1})†	PO_4^{3-} (μmol L^{-1})†	Chlorophyll *a* (μg L^{-1})‡	Leucine incorporation (pmol L^{-1} h^{-1})§
A3-1	19 Jan	52±12	3.5	23±0.4	1.5±0.1	1.6±0.5	77±21
A3-4	04 Feb	79±20	3.6	23±0.0	1.8±0.3	1.5±0.1	30±2
A3-5	12 Feb	84±19	3.9	22±0.4	1.8±0.1	1.0±0.1	41±10
B5	02 Feb	84±16	2.8	25±0.6	1.7±0.1	1.7±0.1	31±2
C11	26 Jan	73±13	2	31±0.2	2.1±0.0	0.2±0.1	13±3

* The wind mixed layers are the mean ± SD of all conductivity, temperature, density casts performed during the occupation of the stations. The mixed-layer depth is based on a difference in sigma of 0.02 to the surface value.
† Mean values ± SD for the mixed-layer depth are given (from Mosseri et al. 2008).
‡ Mean values ± SD for the upper 100 m are given (from Uitz et al. 2009). Chlorophyll *a* concentrations are based on pigment analyses.
§ Mean values ± SD for the upper 100 m are given (from Obernosterer et al. 2008).

nutrient, low-chlorophyll (HNLC) waters (West et al. 2008). Several operational taxonomic units (OTUs) belonging to the major bacterial groups Alphaproteobacteria (the *Roseobacter* OTUs RCA and NAC11-7, and the SAR11 clade), Gammaproteobacteria (the OTUs SAR92 and SAR86), and Bacteroidetes (the OTU Agg58 and a *Polaribacter* OTU) were abundant in clone libraries constructed for contrasting sites in the Kerguelen study region (West et al. 2008). These subgroups are members of the bacterial community in a variety of marine environments; however, only a few studies report on their quantitative contribution to abundance and activity in the polar oceans. The cosmopolitan SAR11 clade contributed up to 27% to bulk bacterial abundance in the Arctic Ocean and in Antarctic coastal waters, where this bacterial group also actively assimilated various organic compounds (Malmstrom et al. 2007; Straza et al. 2010). The *Roseobacter* cluster RCA is reported to have global distribution with particularly high abundances in the Southern Ocean (Selje et al. 2004). The subgroups RCA, SAR86, Agg58, and *Polaribacter* accounted each for up to 12% of bulk abundance in the Arctic Ocean, and *Polaribacter* contributed 10–22% to bulk abundance in coastal Antarctic waters (Malmstrom et al. 2007; Straza et al. 2010). These previous studies provide insight into spatial and temporal patterns of these bacterial groups; however, their ecological implications remain to be investigated.

The objective of the present study was to determine the contribution of the OTUs previously identified for the naturally iron-fertilized region off Kerguelen (West et al. 2008) to bulk abundance and leucine incorporation using the quantitative approach catalyzed reporter deposition–fluorescence in situ hybridization and microautoradiography (MICRO-CARD-FISH). Our results demonstrate that the observed bulk response to the Kerguelen bloom induced by natural iron fertilization was attributable to bacterial groups distinct from those present and active in HNLC waters.

Methods

Study sites—Seawater samples were collected in the core of the spring phytoplankton bloom above the Kerguelen Plateau (Sta. A3) and in off-plateau HNLC waters (Sta. C11) during the KEOPS cruise (19 January–13 February 2005). Based on information obtained from a composite of the Moderate Resolution Imaging Spectroradiometer (MODIS) and the Medium Resolution Spectrometer (MERIS) satellite images, the phytoplankton bloom above the Kerguelen Plateau started early November 2004, thus roughly 2 months prior to the KEOPS cruise (Blain et al. 2007). The bloom site A3 was visited several times, and samples for the present study were collected during the first (A3-1, 19 January), fourth (A3-4, 04 February), and fifth visits (A3-5, 12 February), allowing us to follow temporal changes from the peak of the bloom to its decline (Table 1). Samples were also collected at Sta. B5, located above the Kerguelen Plateau roughly 185 km SE of Sta. A3. As revealed from MODIS and MERIS satellite images, Sta. B5 was characterized by transient high phytoplankton biomass that appeared roughly 1 week prior to our visit at this site. At all stations, concentrations of nitrate and nitrite ($NO_3^- + NO_2^-$) and phosphate (PO_4^{3-}) were relatively high (22–31 μmol L^{-1} and 1.5–2.1 μmol L^{-1}, respectively) and did not display major changes over the 3-week study period (Table 1) (Mosseri et al. 2008). Concentrations of dissolved iron were similar in surface waters above and off the plateau (0.073–0.090 nmol L^{-1}; Blain et al. 2008). However, iron fertilization resulted in an increased vertical flux of iron that stimulated biological activity. Differences between the on- and off-plateau stations were most pronounced for concentrations of chlorophyll *a* that were 1.6 μg L^{-1} and 1.7 μg L^{-1} in surface waters at Sta. A3 and B5, respectively, and 0.2 ± 0.1 μg L^{-1} in the upper 100 m at the HNLC site C11 (Table 1) (Uitz et al. 2009). At Sta. A3, concentrations of chlorophyll *a* decreased to 1.0 μg L^{-1} by the end of the cruise (Fig. 1). Similarly, rates of bulk leucine incorporation were highest in the upper 100 m during the peak of the bloom (77 pmol leucine L^{-1} d^{-1}) and substantially lower at stations outside the bloom (13–31 pmol leucine L^{-1} d^{-1}) and during the decline of the bloom (30–41 pmol leucine L^{-1} d^{-1}) (Table 1) (Obernosterer et al. 2008).

Abundance and activity of bacterial groups—Probe design: Results from previously constructed clone libraries indicated that several bacterial groups were more abundant or specific to Sta. A3 (the OTUs NAC11-7 and RCA

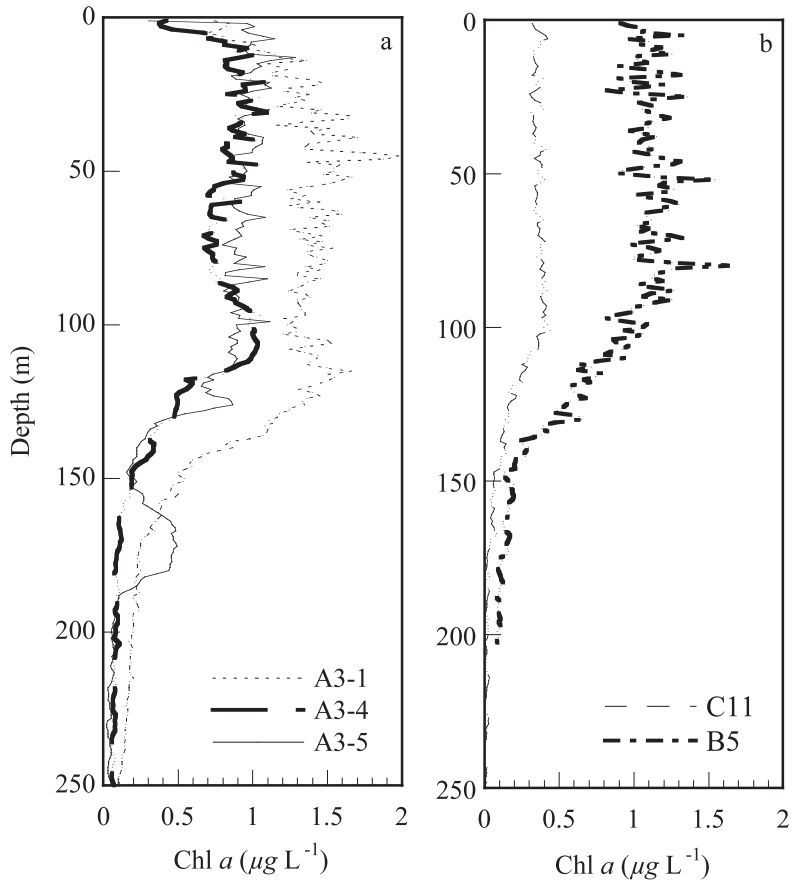

Fig. 1. Depth profiles of concentrations of chlorophyll *a* (Chl *a*) as obtained from in situ fluorescence at Sta. (a) A3, (b) B5 and C11. At Sta. A3 depth profiles for the visits on 19 January (A3-1), 04 February (A3-4), and 12 February (A3-5) are given.

belonging to the *Roseobacter* clade of the Alphaproteobacteria, the OTU SAR92 belonging to the Gammaproteobacteria, and one branch of the Agg58 cluster belonging to the Bacteroidetes) or to Sta. C11 (the SAR11 cluster, the SAR86 cluster, and a *Polaribacter* OTU) (West et al. 2008). To determine the contribution of these bacterial groups to bulk abundance and leucine incorporation, we applied MICRO-CARD-FISH using newly designed probes together with other available probes. Probes were designed for the OTUs NAC11-7, RCA, SAR92, the major *Polaribacter* cluster, and to a cluster affiliated with the previously described branch 1 of the Agg58 cluster (O'Sullivan et al. 2004) (Table 2). We stress that the probes were designed to be specific for the dominant groups revealed in the clone library, and we did not aim to design probes for all members of a given clade or lineage that could be generally applicable to other environments. Therefore, the probes that were selected targeted the maximum number of sequences within our target OTUs while maximizing the number of mismatches with nontarget species in our clone library groups (West et al. 2008) and in the ARB database used. The probes were designed in 2007 using the Probe Design tool of the ARB software package (Ludwig et al. 2004) using the ssujun02 ARB database. A new RCA probe was designed because the probe RCA-825 (Selje et al. 2004) had only one mismatch to the other dominant *Roseobacter* OTU in the clone library, NAC11-7, and the probe Roseo-RCA-845 (Malmstrom et al. 2007) had many out-of-group hits including the NAC11-7 group. Our RCA probe targets a similar region as the probe LE17-998 (Mayali et al. 2008) and has essentially the same specificity. New probes for the major *Polaribacter* cluster and Agg58 cluster detected in our clone libraries were also designed because the previously published probes (Malmstrom et al. 2007) either did not target our groups (Polaribacter-740, Agg58-145) or, in the case of Polaribacter-218, targeted a region where we had little sequence information. We did test the Polaribacter-218 probe in parallel with Polaribacter-865 and both probes gave similar percentage abundances (data not shown). Their specificity was originally verified with the Probe Match tool of the ARB software, the Probe Match tool of the Ribosomal Database Project (Cole et al. 2009), and Blastn, and has been rechecked with a recent Silva database, Silva_104_NR (nonredundant) (Pruesse et al. 2007). A summary of the target range and specificity of the probes is shown in Table 3. When considering the sequence data set from Kerguelen (West et al. 2008), the probes showed zero or fewer than three hits outside of the target group for as many as two mismatches. When the probes

Table 2. Oligonucleotide sequences and target groups for the probes designed in this study.

Probe name*	Probe sequence (5′→3′)	Target OTU in KEOPS library†	Target group in Silva_104_NR
RoseoRCA_992	GTA GTA GCA CAG GAT GTC	*Roseobacter* RCA cluster	*Roseobacter* clade DC5-80-3 lineage
RoseoRCA_975H	AAG GGT TGG TAA GGT TCT		
RoseoRCA_1011H	GGA ACG TAC CAT CTC TG		
Roseo-NAC11-7_1450	GGT TGG CTG CCC CTA TAA	*Roseobacter* NAC11-7 cluster	One cluster within: *Roseobacter* NAC11-7 lineage
SAR92_1279	CGA CCA GCT TTG TGA GAT	SAR92 cluster	SAR92 clade
SAR92_1280C1	CGA CGA GCT TTG TGA GAT		
SAR92_1280C2	CGA CCG GCT TTG TGA GAT		
SAR92_1265H	TAG CTC CCC CTC GCG		
SAR92_1298H	GAC TGC GAT CCG GAC TA		
Polaribacter_836	AGT CAC TGA GCT AAT GCC	*Polaribacter* cluster	One cluster within: *Polaribacter*
Polaribacter_859H	GGT ACT TAT CAC TTT CGG T		
Polaribacter_816H	CAA CAA CTA GTA TCC ATC G		
Agg58_1269	TTA AGG ATT CGC TCC CTG	Agg58 Branch 1	One cluster within: Cryomorphaceae–*Owenweeksia*

* H, helper probes; C, competitor probes.
† OTUs as defined previously (West et al. 2008).

were checked against the Silva_104_NR, there were a few out-of-group hits (Table 3), but these hits were mostly single sequences isolated in different clusters.

For the RCA, SAR92, and *Polaribacter* OTUs, helper probes were designed to improve the fluorescence signal (Fuchs et al. 2000). Additionally, for the SAR92 group, two competitor probes were designed to hybridize to *Shewanella* spp., many of which possessed single mismatches in two different positions to the SAR92_1279 probe.

For the optimization of the hybridization conditions, formamide concentrations (from 45% to 60%) were tested either on cultured representatives (for SAR92 and *Polaribacter* I from the culture collection Microbial Observatory Laboratoire Arago [MOLA]) or on the environmental samples when no cultured representatives were available. For SAR92, the cultured representative MOLA455 (100% identity) was used as a positive control, and MOLA200 (*Shewanella* sp.; one mismatch) as a negative control. For *Polaribacter*, MOLA340 (*Polaribacter dokdonensis*; 100% identity) was used as a positive control and MOLA512 (*Tenacibaculum* sp.; three mismatches) was used as a negative control. Cultures were grown in marine broth at 25°C, harvested in the exponential phase, and fixed in 50% PBS (phosphate buffered saline), 50% ethanol. Fixed cells (3 μL) were spread into wells of 10-well glass slides, dried, and then dehydrated in an ethanol series (50%, 80%, 100%) before carrying out CARD-FISH as described below. The formamide concentration used for SAR92 and *Polaribacter* group was 50%, and the formamide concentration used for all other probes was 55%.

To target the SAR11 and SAR86 clusters, we used the probes SAR11-152R, SAR11-441R, SAR11-542R, SAR11-732R (Morris et al. 2002), and the probe SAR86 (Eilers et al. 2000), respectively. The probes Eub338-I, -II, and -III (Daims et al. 1999) were used for the identification of most Bacteria and the Eub338-I antisense probe Non338 was used to determine nonspecific binding. The proportion of cells that hybridized with the combined probes Eub338-I, -II, and -III and the probe NON338 was 75 ± 12% and 1 ± 2% (mean ± SD, n = 16) of the diamidino-2-phenylindole (DAPI)–stained cells. The sum of the relative abundances of the bacterial groups NAC11-7, RCA, SAR11, SAR92, and SAR86 roughly equaled the relative abundance determined by the respective general probes Alphaproteobacteria (mean ± SD, 117 ± 30%, n = 6, data not shown) and Gammaproteobacteria (mean ± SD, 120 ± 11% of DAPI-stained cells, n = 3, data not shown). By contrast, the sum of Agg58 and *Polaribacter* I accounted for 50 ± 19% and 21 ± 7% of cells identified as Bacteroidetes (mean ± SD, each n = 3, data not shown), indicating that Bacteroidetes was the least identified group by the probes applied.

MICRO-CARD-FISH: To determine the relative contribution of the bacterial groups to abundance and

Table 3. Specificity of the probes for the entire Kerguelen sequence data set or for the Silva_104_NR database.

Probe	No. sequences in KEOPS OTU	In-group hits	Out-of-group hits (Kergeulen data set) for different mismatches			No. sequences in Silva_104_NR target group	In-group hits	Out-of-group hits (0 mismatch)
			0	1	2			
RoseoRCA_992	28	28	0	0	0	123	119	14
Roseo-NAC11-7_1450	30	30	0	0	0	172	49	5
SAR92_1279	33	33	0	0	3	98	87	11
Polaribacter_836	26	24	0	0	0	129	66	3
Agg58_1269	29	29	0	0	1	185	54	1

leucine incorporation, we applied MICRO-CARD-FISH. Our CARD-FISH protocol is based on that described in Sekar et al. (2003), and we followed the protocol of Cottrell and Kirchman (2000) for the microautoradiographic development. Raw seawater samples (20–50 mL) were incubated with [4,5-^{3}H]leucine (Amersham; specific activity 160 Ci mmol^{-1}) at a final concentration of 20 nmol L^{-1} in the dark at in situ temperature for 2–4 h. Controls were fixed with paraformaldehyde (PFA; 2% final concentration) 10 min prior to incubation with [^{3}H]leucine. The incubations were terminated by adding PFA (2% final concentration), and after storage at 4°C in the dark for 12 h, samples were filtered onto 0.2-μm polycarbonate filters (25-mm filter diameter, Nuclepore). Filters were stored at −20°C until treated. Briefly, for CARD-FISH, filters were embedded in low-melting-point agarose (0.2% final concentration), dried, dehydrated (96% ethanol, 1 min) and treated with lysozyme (Fluka; 10 mg mL^{-1}, 100 mmol L^{-1} Tris [pH 8], 50 mmol L^{-1} ethylenediaminetetraacetic acid) for 1 h at 37°C to allow cell wall permeabilization. The filters were subsequently washed in Milli-Q water and dehydrated in ethanol (96%) for 1 min. Probe working solution was added at a final concentration of 2.5 ng μL^{-1} and the hybridization was done at 35°C for 2 h.

For the microautoradiographic development, the previously hybridized filter sections were placed onto slides coated with photographic emulsion (type NTB-2, Kodak; diluted 1 : 1 with Milli-Q water). The photographic emulsion was heated at 43°C for 30–60 min before utilization. The slides were then dried (for 15 min) on an ice-cold aluminum plate and kept in a dark box during exposure at 4°C. The slides were developed for 2 min (Dektol developer [1 : 1 dilution with Milli-Q water], Kodak), rinsed with Milli-Q water for 10 s, fixed for 6 min (Fixer Tmax, Kodak), and again rinsed for 6 min in Milli-Q water. After having dried the slides in a desiccator for 12 h, filter sections were peeled off and the cells were counterstained with a DAPI mix (4 parts Citifluor, 1 part Vectashield [Vector Laboratories] with DAPI at a final concentration of 0.5 μg mL^{-1}). Time series were performed for surface water samples at Sta. A3, B5, and C11 to determine the appropriate exposure time. Therefore, slides were developed after 12, 24, 36, 48, 72, and 96 h. The maximum percentage of DAPI-stained cells associated with silver grains was obtained after 48 h at Sta. A3 and B5, and after 72 h at Sta. C11. The slides were examined under an Olympus AX70 epifluorescence microscope and an image analysis system as described in Cottrell and Kirchman (2000). For each slide, 10–20 fields were enumerated. To determine the contribution of different bacterial groups to leucine incorporation, the number of probe-positive cells associated with silver grains was divided by the number of DAPI-stained cells associated with silver grains. Replicate filter pieces (n = 3–5) were prepared and counted for all probes applied in the present study. Results are presented as mean values ± standard deviation of replicate filter pieces. Absolute cell numbers were calculated by using the total DAPI counts and the flow cytometry data reported previously (Obernosterer et al. 2008).

Results

Relative abundance of bacterial groups at two contrasting sites—Pronounced differences in the relative abundance of the specific bacterial groups investigated were detectable between surface waters of the bloom Sta. A3-1 and the HNLC site C11 (Fig. 2a,b). The probes used in the present study were designed to target the major OTUs identified in previously constructed clone libraries for A3 (at 120 m) and at C11 (at 100 m). At the bloom station, at 120 m, Alphaproteobacteria were dominated by the two *Roseobacter* groups NAC11-7 and RCA accounting for 17 ± 3% (mean ± SD, n = 4) and 17 ± 4% (mean ± SD, n = 3) of DAPI-stained cells, respectively, while the contribution of SAR11 to DAPI-stained cells was 6 ± 2% (mean ± SD, n = 3) (Fig. 2a). Within the Gammaproteobacteria SAR92 had a markedly higher contribution to bulk abundance than SAR86 (21 ± 1% and 5 ± 3% of DAPI-stained cells, respectively; mean ± SD, n = 3). The two Bacteroidetes groups Agg58 and *Polaribacter* accounted for 11 ± 4% and 6 ± 2% of DAPI-stained cells (mean ± SD, n = 3) at 120 m, respectively. At 5 m and 50 m, SAR92, Agg58, and *Polaribacter* revealed similar relative abundances than at 120 m (mean of 5 m and 50 m 21%, 9%, and 7% of DAPI-stained cells, respectively). By contrast, the relative abundances of NAC11-7 and RCA decreased markedly, each accounting for < 4% of DAPI-stained cells at 5 m and 50 m (Fig. 2a). At the HNLC site C11, SAR11 was a dominant group in the upper 100 m, accounting for 37 ± 9% of DAPI-stained cells (mean ± SD of 10 m, 80 m, and 100 m) (Fig. 2b). In contrast to the bloom station, the relative abundance of the *Roseobacter* groups NAC11-7 and RCA remained low at all depths (2 ± 3% and 6 ± 2%, respectively, mean ± SD of 10 m, 80 m, and 100 m). Also in contrast to the bloom station, the relative abundance of SAR92 was < 3% of DAPI-stained cells at Sta. C11. SAR86 accounted for 5–12% of DAPI-stained cells at the HNLC site in the upper 100 m. The relative abundance of Agg58 was low at C11 (< 2% of DAPI-stained cells) and *Polaribacter* revealed relative abundances ranging between 3% and 6% in the upper 100 m.

At the depths where the clone libraries were constructed for probe design, 83% (at 120 m for A3) and 61% (at 100 m at C11) of bulk bacterial abundance could be identified by the 10 probes for the seven bacterial groups targeted in the present study. Only at the bloom site A3, these percentages decreased in the upper water layers (to 49% and 58% of DAPI-stained cells at 5 m and 50 m, respectively), while at C11 the 10 probes accounted for 61 ± 6% of DAPI-stained cells throughout the upper 100 m. At both sites, the specific probes applied yielded low percentages at 200 m (10–21% of DAPI-stained cells, n = 2).

Relative contribution of bacterial groups to leucine incorporation at two contrasting sites—Overall, the relative contribution of the bacterial groups to bulk leucine incorporation revealed a similar pattern as that observed for their contribution to abundance (Fig. 2d,e). At the bloom site A3, the *Roseobacter* groups NAC11-7 and RCA, SAR92, and Agg58 were the most important contributors

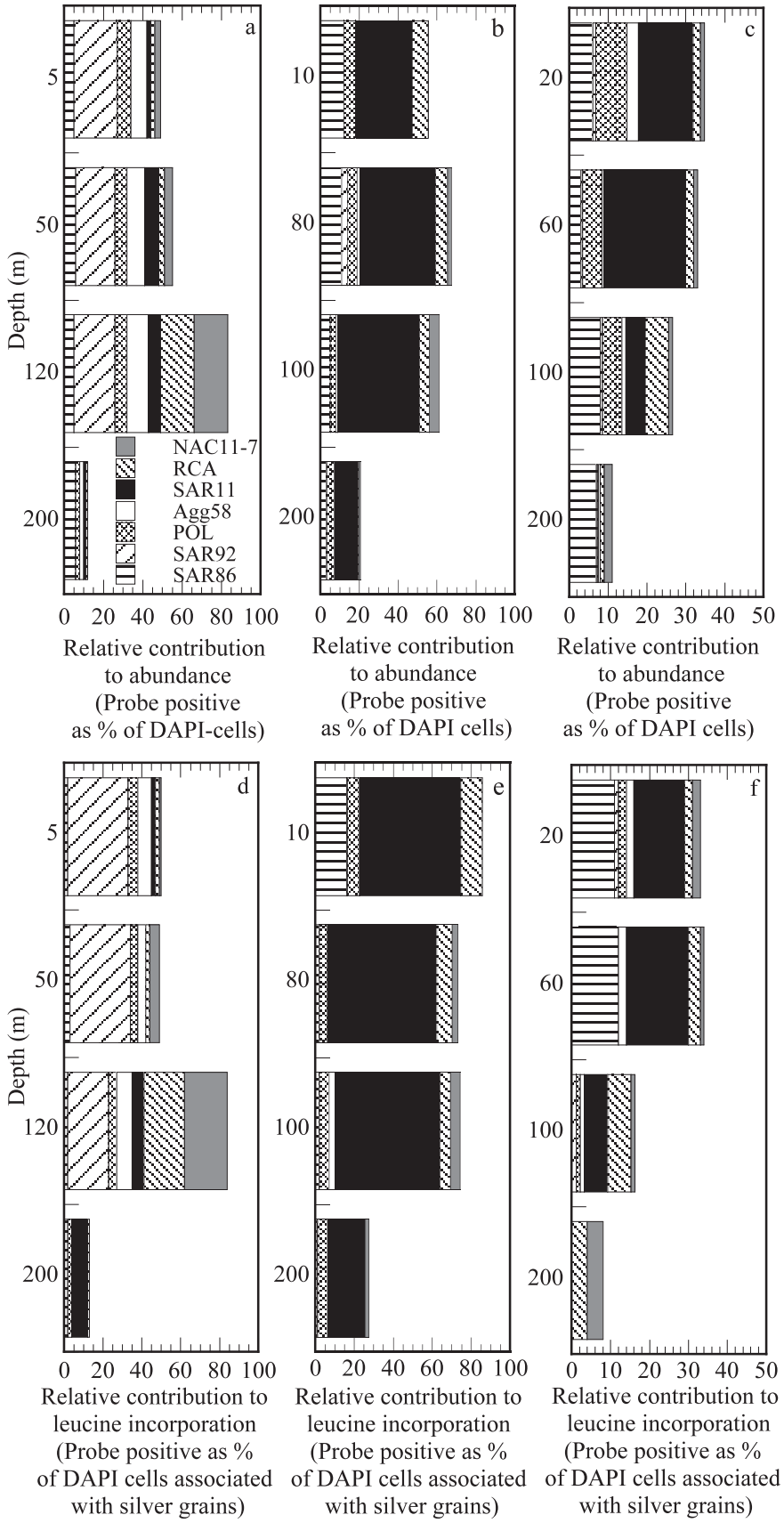
a
b
c
d
e
f
Depth (m)
5
50
120
200
10
80
100
20
60
NAC11-7
RCA
SAR11
Agg58
POL
SAR92
SAR86
0 20 40 60 80 100
0 10 20 30 40 50
Relative contribution to abundance (Probe positive as % of DAPI-cells)
Relative contribution to abundance (Probe positive as % of DAPI cells)
Relative contribution to leucine incorporation (Probe positive as % of DAPI cells associated with silver grains)

to bulk leucine incorporation in the upper 120 m, together explaining 47–82% of DAPI-stained cells incorporating leucine. By contrast, at the HNLC site C11 SAR11 was the dominant contributor to bulk leucine incorporation (mean ± SD, 54 ± 2% of DAPI-stained cells incorporating leucine, $n = 3$) in the upper 100 m, with lower contributions of the groups RCA (mean ± SD, 8 ± 3%, $n = 3$), SAR86 (mean ± SD, 7 ± 8%, $n = 3$), and *Polaribacter* (mean ± SD, 4 ± 2%, $n = 3$).

Presence and activity of bacterial groups during a transient phytoplankton bloom—Sta. B5 was characterized by a sudden development of high phytoplankton biomass over the time period of roughly 1 week at the beginning of the KEOPS cruise, as revealed by real-time MODIS–MERIS satellite images. Applying the specific probes revealed a pattern similar to that observed at the HNLC site C11 (Fig. 2c,f). The most dominant contributors to abundance and leucine incorporation were SAR11 and SAR86 (13 ± 8% and 12 ± 5%, 6 ± 3% and 8 ± 7% of DAPI-stained cells and DAPI-stained cells incorporating leucine, respectively, $n = 3$). *Polaribacter* was abundant (6 ± 2%, $n = 3$) in the upper 100 m, but exhibited a low contribution to leucine incorporation (< 2% of DAPI-stained cells incorporating leucine). At Sta. B5, our specific probes accounted for 31 ± 4% and 27 ± 10% of DAPI-stained cells and DAPI-stained cells incorporating leucine, respectively, in the upper 100 m.

Temporal changes of the abundance and activity of bacterial groups at the bloom site—Sta. A3 was visited three times (*see* Table 1), allowing us to follow the bloom from its peak to its decline (Fig. 3). In contrast to our first visit that revealed high relative abundances of the *Roseobacter* OTUs NAC11-7 and RCA at the depth where high phytoplankton biomass accumulated (7×10^7 cells L^{-1} at 120 m), these bacterial groups were almost undetectable during the following visits (range 0.05–3×10^7 cells L^{-1}) (Fig. 3a,b). By contrast, the abundance of SAR11 in the upper 120 m increased from $2.3 \pm 1.3 \times 10^7$ cells L^{-1} ($n = 3$) up to 10×10^7 cells L^{-1} during our third visit (Fig. 3c). Similar SAR11 abundances were determined at the HNLC site ($9.3 \pm 2.1 \times 10^7$ cells L^{-1}, $n = 3$). Interestingly, the abundance of SAR86 markedly increased in the upper 50 m from $2.5 \pm 0.3 \times 10^7$ cells L^{-1} ($n = 5$) to up to 8.6×10^7 cells L^{-1} only at the end of the bloom (Fig. 3d). The abundance of SAR86 at the HNLC site was $2.3 \pm 1 \times 10^7$ cells L^{-1} ($n = 3$). The most striking observation was the decrease of SAR92 from $10 \pm 1 \times 10^7$ cells L^{-1} ($n = 3$) during our first visit to Sta. A3 to $5 \pm 1 \times 10^7$ cells L^{-1} ($n = 2$) 16 d later and the disappearance of this group during our third visit that coincided with the decline of the phytoplankton bloom ($0.4 \pm 0.6 \times 10^7$ cells L^{-1}, $n = 3$) (Fig. 3e). The Bacteroidetes groups Agg58 and *Polaribacter* displayed similar patterns, though less pronounced. The abundances of Agg58 and *Polaribacter* were highest during our first visit at Sta. A3 (4.4 ± 0.4 and $3.0 \pm 0.5 \times 10^7$ cells L^{-1}, respectively, $n = 3$ each) than on all other sampling occasions at this site (range for Agg58 0.03–2.7×10^7 cells L^{-1} and for *Polaribacter* 0.02–1.3×10^7 cells L^{-1}) (Fig. 3f,g). The abundances of Agg58 and *Polaribacter* were $0.2 \pm 0.2 \times 10^7$ cells L^{-1} and $1.2 \pm 0.3 \times 10^7$ cells L^{-1}, respectively, at the HNLC site C11. This temporal pattern observed in the abundance of the bacterial groups was overall also reflected in their relative contribution to leucine incorporation (data not shown). During our last visit to Sta. A3, the bacterial groups targeted by the newly designed probes accounted together for much smaller fractions of the bulk abundance (32 ± 9% of DAPI-stained cells, $n = 4$) and leucine incorporation (28 ± 7% of DAPI-stained cells incorporating leucine, $n = 4$).

Pooling the results from all stations and depths, the relative contribution of the bacterial groups to bulk abundance and leucine incorporation was significantly correlated (Spearman, $r = 0.927$, $p < 0.001$, $n = 160$). Except for SAR86, each group individually revealed a significant relationship between its relative contribution to abundance and leucine incorporation ($p < 0.05$, $n = 16$ for each group). It is noteworthy that SAR92 (at Sta. A3-1) and SAR11 (at Sta. C11) revealed both higher relative contributions to leucine incorporation (30% and 54% of DAPI-stained cells incorporating leucine, respectively) than to bulk abundance (20% and 37% of DAPI cells, respectively) (Fig. 2).

Discussion

Our results demonstrate that a few bacterial groups identified as clusters of ≥ 99% identity of the 16S ribosomal ribonucleic acid (rRNA) gene account for a substantial part of bulk abundance and leucine incorporation during a phytoplankton bloom induced by natural iron fertilization in the Southern Ocean. These bacterial groups were distinct from those present and active in HNLC waters. The observed pronounced patterns of the bacterial groups associated with different phases or depth layers of the Kerguelen bloom could provide novel information on their potential functional roles and how this could affect ocean carbon and iron biogeochemistry.

The two *Roseobacter* groups NAC11-7 and RCA revealed both a distinct vertical distribution with particularly high contributions to abundance and leucine incorporation at 120 m during the peak of the Kerguelen bloom (Fig. 2). A subsurface maximum of phytoplankton biomass characterized this depth layer as indicated by roughly 2- and 4-fold higher concentrations of chlorophyll *a* (Uitz et

←

Fig. 2. Relative contribution of bacterial groups to bulk abundance and leucine incorporation in the core of the bloom at (a, d) Sta. A3-1, (b, e) at the HNLC site C11, and (c, f) at Sta. B5. Groups not presented at 200 m were not detectable. Note different scale on x-axis of Fig. 2c and 2f. POL, *Polaribacter* group.

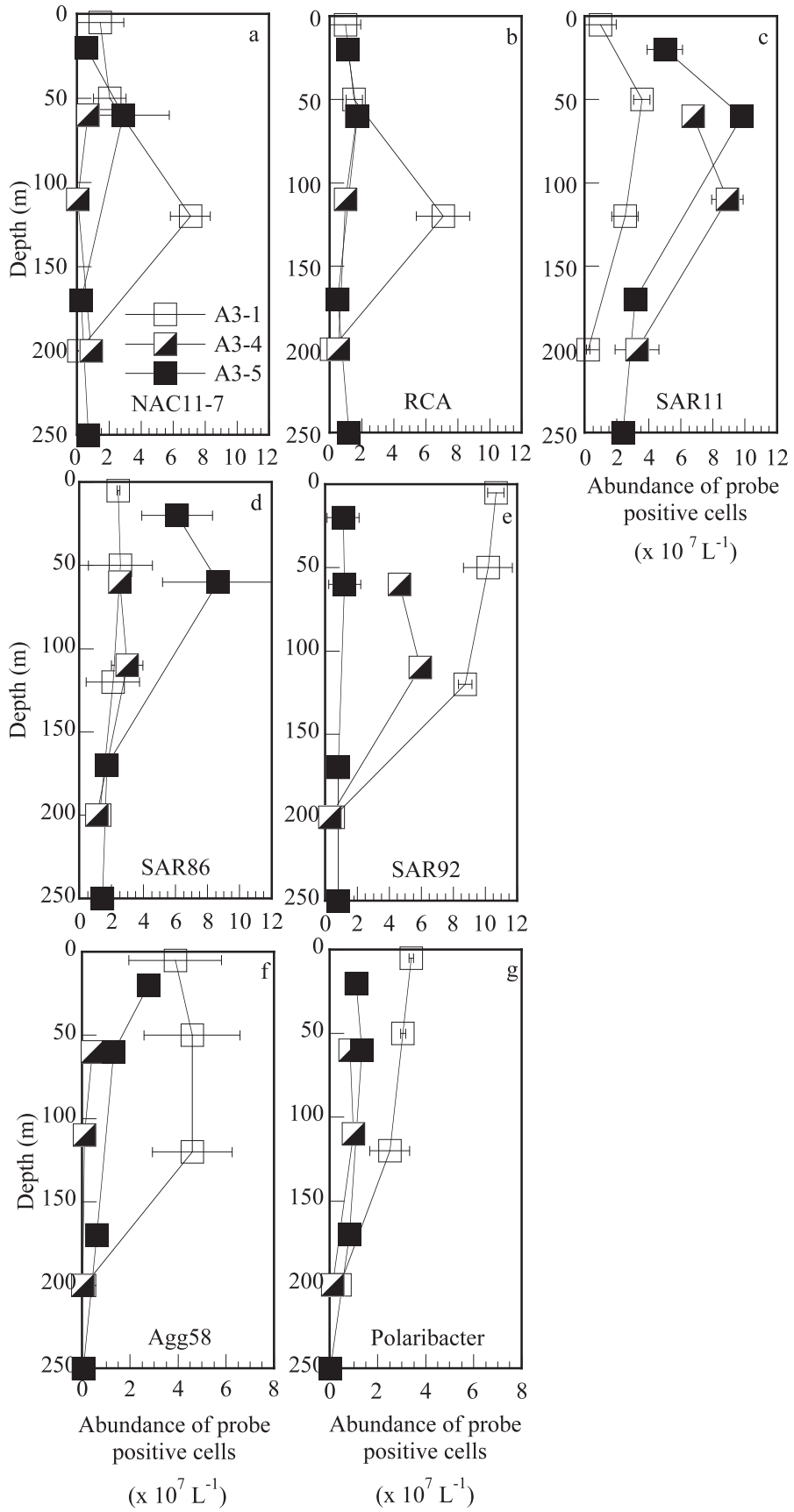

Fig. 3. Temporal changes in the abundance of bacterial groups at the bloom site A3. Groups not presented at 200 m were not detectable. Mean values ± SD of triplicate filter pieces are given.

al. 2009) and biogenic silica (Mosseri et al. 2008), respectively, than in the upper 50-m water layer. Underwater video profiles further revealed that this subsurface maximum was dominated by large particles (0.5 cm < equivalent spherical diameter < 3.34 cm) (Jouandet et al. 2011), composed of aggregated sinking diatoms and fecal pellets (Armand et al. 2008; Ebersbach and Trull 2008). The high abundance and activity of the *Roseobacter* OTUs NAC11-7 and RCA well below the euphotic zone let us hypothesize that these groups could contribute to the degradation of cellular material from decaying diatom cells. A similar conclusion was drawn recently for the RCA group from a study performed in the coastal North Sea (Giebel et al. 2011).

A pattern contrasting to that of the *Roseobacter* OTUs NAC11-7 and RCA was observed for SAR92 belonging to Gammaproteobacteria and the Bacteroidetes OTU Agg58, as these groups were present and active throughout the upper 120 m at the bloom site A3 (Fig. 2). The depth distribution of SAR92 and Agg58 in terms of abundance and activity was similar to that of the total bacterial abundance and leucine incorporation (Obernosterer et al. 2008). Together SAR92 and Agg58 accounted for roughly 40% of bulk leucine incorporation that was shown to be about 6-fold higher in surface waters at the bloom site as compared to HNLC waters (Table 1). The high abundance and activity of SAR92 in surface waters at Sta. A3 suggests that this OTU is competitive at high nutrient concentrations and concurrent high dissolved organic matter (DOM) supply. This idea is in part supported by the observation that SAR92 was responsive to phytoplankton blooms induced by inorganic nutrient enrichment in microcosm experiments (Pinhassi et al. 2005). Further, several strains belonging to the SAR92 clade were isolated in the nutrient-rich upwelling off the Oregon coast, where this clade accounted for up to 10% of bulk bacterial abundance (Stingl et al. 2007). It was interesting to note that within the euphotic layer of the Kerguelen bloom, the relative contribution of SAR92 to leucine incorporation (30%) was higher than its contribution to abundance (20%) (Fig. 2a,d). The enhanced activity of SAR92 in surface waters could possibly be linked to the presence of proteorhodopsin, as suggested previously (Stingl et al. 2007). In the Western Arctic Peninsula, the subgroup ANT4D3 dominated Gammaproteobacteria (Straza et al. 2010). This group was also present in our clone libraries from Sta. A3 and C11, but at lower relative abundances (West et al. 2008). There is evidence that members belonging to Bacteroidetes could play an important role in the degradation of complex organic compounds (Cottrell and Kirchman 2000). It remains a challenging question whether the contrasting spatial and temporal distribution of the two Bacteroidetes OTUs Agg58 and *Polaribacter* observed in the present study could reflect qualitative differences of bioavailable DOM.

The OTUs SAR92, Agg58, RCA, and NAC11-7 dominated abundance and leucine incorporation during the peak of the Kerguelen bloom, but they disappeared toward the decline of the bloom, when cosmopolitan groups like SAR11 and SAR86 became more abundant (Fig. 3). This pattern was particularly pronounced for the OTU SAR92. Interestingly, the bacterial groups associated with the bloom at Sta. A3 were absent from Sta. B5. This site was characterized by high phytoplankton biomass that appeared roughly 1 week prior to our visit at this station, and by relatively low rates of bulk bacterial leucine incorporation (Table 1). These observations suggest that the bacterial groups present and active during the peak of the Kerguelen bloom that had an overall duration of about 3 months were well adapted to the environmental conditions. A tight correlation between the relative contributions of the different bacterial groups to leucine incorporation and their respective contributions to abundance, as observed in the present study, were suggested to be indicative for bottom-up control (Cottrell and Kirchman 2003). Indeed, heterotrophic nanoflagellates exerted a weak top-down control on heterotrophic bacteria at the bloom site (Christaki et al. 2008). The possible acclimatization of the bacterial community to the environmental conditions within the Kerguelen bloom could in part explain the enhanced bulk metabolic response to natural iron fertilization in the Southern Ocean.

During the Kerguelen bloom, both carbon and iron were likely driving factors for bacterial heterotrophic metabolism and also community composition. A major difference of the bloom site A3 to the HNLC site was the enhanced DOM supply due to the higher rates of primary production and phytoplankton biomass (Table 1). By contrast, concentrations of major inorganic nutrients (Table 1) and dissolved iron revealed similar spatial distribution (Blain et al. 2008). Thus, the enhanced DOM supply by phytoplankton primary production constituted most likely one mechanism that selected for specific bacterial groups. One driving factor could be the chemical composition of the DOM produced by the different phytoplankton species dominating at our study sites, *Chaetoceros* subgenus *Hyalochaete* spp. and *Eucampia antarctica* at the peak and at the decline of the Kerguelen bloom, respectively, and *Fragilariopsis pseudonana* and *F. kerguelensis* at the HNLC site (Armand et al. 2008). Several previous studies have suggested such an association between phytoplankton and bacteria, based on the investigation of the bacterial community composition associated to various phytoplankton blooms or the bacterial growth on algal-derived DOM (van Hannen et al. 1999; Rink et al. 2007).

Most likely independent of the chemical composition of DOM, the processing of an enhanced supply of organic carbon by bacteria requires iron. The cellular Fe : C quota of heterotrophic bacteria has been estimated at 7.5 μmol Fe (mol C)$^{-1}$ and is thus about 2-fold higher than that of microphytoplankton (Tortell et al. 1996). For the bloom Sta. A3, we estimated that heterotrophic bacteria were the second most important iron consumers above the Kerguelen Plateau (Obernosterer et al. 2008). A short-term (day) iron budget indicated that the high biological iron requirements at Sta. A3 were not met by the supply of iron from below (Blain et al. 2007). This suggests that access to not directly available iron is of critical importance to maintain the observed high metabolic activity. Siderophores enhance the solubility of iron in seawater, and

heterotrophic bacteria are known to be their dominant producers (Gledhill et al. 2004). The question, however, whether siderophore production is specific to some bacterial groups and whether this physiological trait could represent a selective advantage remains to be investigated.

In the present study, the use of a combination of several probes targeting narrow phylogenetic clades defined here as clusters of ≥ 99% identity of the 16S rRNA gene within each of the major bacterial groups allowed us to describe their distinct spatial and temporal patterns in terms of abundance and activity. The bacterial groups identified in the present study contributed substantially to the bacterially mediated carbon cycling in response to natural iron fertilization of the Southern Ocean, highlighting their ecological and biogeochemical importance. The mode of iron fertilization and the duration of the Kerguelen bloom are probably tightly linked to the pronounced response of heterotrophic bacterial activity driven by distinct bacterial groups, emphasizing the value of naturally iron-fertilized regions as in situ laboratories for future studies of the coupling of carbon and iron in the ocean.

Acknowledgments

We thank the principal investigator of the Kerguelen Ocean and Plateau Compared Study (KEOPS) S. Blain, the chief scientist B. Quéguiner, Commandant Heinrich and his crew, and the scientific personnel for their enthusiasm and support aboard the Research Vessel *Marion Dufresne II*. We are grateful to S. Blain, two anonymous reviewers, and M. Zubkov for their constructive criticism on a previous version of this manuscript. Financial support for this work came from the French National program Processus Biogéochimiques dans l'Océan et Flux (PROOF) of the Institut National du Science de l'Univers (INSU) of the Centre National de la Recherche Scientifique (CNRS), the Pierre Fabre, CNRS, Université Pierre et Marie Curie (UPMC) joint research team, and the Institut Polaire Emile Victor (IPEV). We thank Matt Cottrell for his help in the implementation of the image analysis system on our microscopic equipment.

References

Armand, L., V. Cornet-Barthaux, J. Mosseri, and B. Quéguiner. 2008. Late summer diatom biomass and community structure on and around the naturally iron-fertilized Kerguelen Plateau in the Southern Ocean. Deep-Sea Res. II **55:** 653–676, doi:10.1016/j.dsr2.2007.12.031

Arrieta, J. M., M. Weinbauer, C. Lute, and G. Herndl. 2004. Response of bacterioplankton to iron fertilization in the Southern Ocean. Limnol. Oceanogr. **49:** 799–808, doi:10.4319/lo.2004.49.3.0799

Blain, S., and others. 2007. Effect of natural iron fertilization on carbon sequestration in the Southern Ocean. Nature **446:** 1070–1075, doi:10.1038/nature05700

———, G. Sarthou, and P. Laan. 2008. Distribution of dissolved iron during the natural iron-fertilization experiment KEOPS (Kerguelen Plateau, Southern Ocean). Deep-Sea Res. II **55:** 594–605, doi:10.1016/j.dsr2.2007.12.028

———, P. Tréguer, S. Belviso, E. Bucciarelli, M. Denis, S. Desabre, M. Fiala, V. M. Jezequel, J. Le Fevre, P. Mayzaud, J.-C. Marty, and Suzanne Razouls. 2001. A biogeochemical study of the island mass effect in the context of the iron hypothesis: Kerguelen Islands, Southern Ocean. Deep-Sea Res. I **48:** 163–187, doi:10.1016/S0967-0637(00)00047-9

Boyd, P. W., and others. 2007. Mesoscale iron enrichment experiments 1993–2005: Synthesis and future directions. Science **315:** 612–617, doi:10.1126/science.1131669

Christaki, U., I. Obernosterer, F. V. Wambeke, M. Veldhuis, N. Garcia, and P. Catala. 2008. Microbial food web structure in a naturally iron-fertilized area in the Southern Ocean (Kerguelen Plateau). Deep-Sea Res. II **55:** 706–719, doi:10.1016/j.dsr2.2007.12.009

Cole, J., and others. 2009. The Ribosomal database project: Improved alignments and new tools for rRNA analysis. Nucleic Acids Res. **37:** D141–D145, doi:10.1093/nar/gkn879

Cottrell, M., and D. Kirchman. 2000. Natural assemblages of marine proteobacteria and members of the Cytophaga-Flavobacter cluster consuming low-and high-molecular-weight dissolved organic matter. Appl. Environ. Microbiol. **66:** 1692–1697, doi:10.1128/AEM.66.4.1692-1697.2000

———, and ———. 2003. Contribution of major bacterial groups to bacterial biomass production (thymidine and leucine incorporation) in the Delaware estuary. Limnol. Oceanogr. **48:** 168–178, doi:10.4319/lo.2003.48.1.0168

Daims, H., A. Brühl, R. Amann, K. Schleifer, and M. Wagner. 1999. The domain-specific probe EUB 338 is insufficient for the detection of all bacteria: Development and evaluation of a more comprehensive probe set. Syst. Appl. Microbiol. **22:** 434–444.

Ebersbach, F., and T. Trull. 2008. Sinking particle properties from polyacrylamide gels during KEOPS: Controls on carbon export in an area of persistent natural iron inputs in the Southern Ocean. Limnol. Oceanogr. **53:** 212–224, doi:10.4319/lo.2008.53.1.0212

Eilers, H., J. Pernthaler, F. O. Glöckner, and R. Amann. 2000. Culturability an in situ abundance of pelagic bacteria from the north sea. Appl. Environ. Microbiol. **66:** 3044–3051, doi:10.1128/AEM.66.7.3044-3051.2000

Fuchs, B., F. Gloeckner, J. Wulf, and R. Amann. 2000. Unlabeled helper oligonucleotides increase the in situ accessibility to 16S rRNA of fluorescently labeled oligonucleotide probes. Appl. Environ. Microbiol. **66:** 3603–3607, doi:10.1128/AEM.66.8.3603-3607.2000

Giebel, H., D. Kalhoefer, A. Lemke, S. Thole, R. Gahl-Janssen, M. Simon, and T. Brinkhoff. 2011. Distribution of Roseobacter RCA and SAR11 lineages in the North Sea and characteristics of an abundant RCA isolate. ISME J **5:** 8–19, doi:10.1038/ismej.2010.87

Gledhill, M., P. McCormack, S. Ussher, E. Achterberg, R. Mantoura, and P. Worsfold. 2004. Production of siderophore type chelates by mixed bacterioplankton populations in nutrient enriched seawater incubations. Mar. Chem. **88:** 75–83, doi:10.1016/j.marchem.2004.03.003

Jickells, T., and others. 2005. Global iron connections between desert dust, ocean biogeochemistry, and climate. Science **308:** 67–71, doi:10.1126/science.1105959

Jouandet, M., T. Trull, L. Guidi, M. Picheral, F. Ebersbach, L. Stemmann, and S. Blain. 2011. Optical imaging of mesopelagic particles indicates deep carbon flux beneath a natural iron fertilized bloom in the Southern Ocean. Limnol. Oceanogr. **56:** 1130–1140, doi:10.4319/lo.2011.56.3.1130

Ludwig, W., O. Strunk, R. Westram, L. Richter, and H. Meier. 2004. ARB: A software environment for sequence data. Nucleic Acids Res. **32:** 1363–1371, doi:10.1093/nar/gkh293

Malmstrom, R., T. Straza, M. Cottrell, and D. Kirchman. 2007. Diversity, abundance, and biomass production of bacterial groups in the western Arctic Ocean. Aquat. Microb. Ecol. **47:** 45–55, doi:10.3354/ame047045

Mayali, X., P. J. Franks, and F. Azam. 2008. Cultivation and ecosystem role of a marine Roseobacter clade-affiliated cluster bacterium. Appl. Environ. Mirobiol. **74:** 2595–2603, doi:10.1128/AEM.02191-07

Morris, M., M. Rappé, S. Connon, K. Vergin, W. Siebold, C. Carlson, and S. Giovannoni. 2002. SAR11 clade dominates ocean surface bacterioplankton communities. Nature **420:** 806–810, doi:10.1038/nature01240

Mosseri, J., B. Quéguiner, L. Armand, and V. Cornet-Barthaux. 2008. Impact of iron on silicon utilization by diatoms in the Southern Ocean: A case study of Si/N cycle decoupling in a naturally iron-enriched area. Deep-Sea Res. II **55:** 801–819, doi:10.1016/j.dsr2.2007.12.003

Obernosterer, I., U. Christaki, D. Lefèvre, P. Catala, F. V. Wambeke, and P. Lebaron. 2008. Rapid bacterial mineralization of organic carbon produced during a phytoplankton bloom induced by natural iron fertilization in the Southern Ocean. Deep-Sea Res. II **55:** 777–789, doi:10.1016/j.dsr2.2007.12.005

O'Sullivan, L. A., K. E. Fuller, E. M. Thomas, C. M. Turley, J. C. Fry, and A. J. Weightman. 2004. Distribution and culturability of the uncultivated 'AGG58 cluster' of the Bacteroidetes phylum in aquatic environments. FEMS Microb. Ecol. **47:** 359–370, doi:10.1016/S0168-6496(03)00300-3

Pinhassi, J., R. Simo, J. M. Gonzalez, M. Vila, L. Alonso-Saez, R. P. Kiene, M. A. Moran, and C. Pedros-Alio. 2005. Dimethylsulfoniopropionate turnover is linked to the composition and dynamics of the bacterioplankton assemblage during a microcosm phytoplankton bloom. Appl. Environ. Microbiol. **71:** 7650–7660, doi:10.1128/AEM.71.12.7650-7660.2005

Pollard, R., and others. 2009. Southern Ocean deep-water carbon export enhanced by natural iron fertilization. Nature **457:** 577–581, doi:10.1038/nature07716

Pruesse, E., C. Quast, K. Knittel, B. Fuchs, W. Ludwig, J. Peplies, and F. O. Glöckner. 2007. SILVA: a comprehensive online resource for quality checked and aligned ribosomal RNA sequence data compatible with ARB. Nucl. Acids Res. **35:** 7188–7196, doi:10.1093/nar/gkm864

Rink, B., S. Seeberger, T. Martens, C. Duerselen, M. Simon, and T. Brinkhoff. 2007. Effects of phytoplankton bloom in a coastal ecosystem on the composition of bacterial communities. Aquat. Microb. Ecol. **48:** 47–60, doi:10.3354/ame048047

Sekar, R., A. Pernthaler, J. Pernthaler, F. Warnecke, T. Posch, and R. Amann. 2003. An improved protocol for quantification of freshwater Actinobacteria by fluorescence in situ hybridization. Appl. Environ. Microbiol. **69:** 2928–2935, doi:10.1128/AEM.69.5.2928-2935.2003

Selje, N., M. Simon, and T. Brinkhoff. 2004. A newly discovered Roseobacter cluster in temperate and polar oceans. Nature **427:** 445–448, doi:10.1038/nature02272

Stingl, U., R. Desiderio, J. Cho, K. Vergin, and S. Giovannoni. 2007. The SAR92 Clade: An abundant coastal clade of culturable marine bacteria possessing proteorhodopsin. Appl. Environ. Microbiol. **73:** 2290–2296, doi:10.1128/AEM.02559-06

Straza, T., H. Ducklow, A. E. Murray, and D. Kirchman. 2010. Abundance and single-cell activity of bacterial groups in Antarctic coastal waters. Limnol. Oceanogr. **55:** 2526–2536, doi:10.4319/lo.2010.55.6.2526

Tortell, P., M. Maldonado, and N. Price. 1996. The role of heterotrophic bacteria in iron-limited ocean ecosystems. Nature **383:** 330–332, doi:10.1038/383330a0

Uitz, J., H. Claustre, F. Griffiths, J. Ras, N. Garcia, and V. Sandroni. 2009. A phytoplankton class-specific primary production model applied to the Kerguelen Islands region (Southern Ocean). Deep-Sea Res. I **56:** 541–560, doi:10.1016/j.dsr.2008.11.006

van Hannen, E., W. Mooij, M. P. V. Agterveld, H. J. Gons, and H. J. Laanbroek. 1999. Detritus-dependent development of the microbial community in an experimental system: Qualitative analysis by denaturating gradient gel electrophoresis. Appl. Environ. Microbiol. **65:** 2478–2484.

West, N., I. Obernosterer, O. Zemb, and P. Lebaron. 2008. Major differences of bacterial diversity and activity inside and outside of a natural iron-fertilized phytoplankton bloom in the Southern Ocean. Environ. Microbiol. **10:** 738–756, doi:10.1111/j.1462-2920.2007.01497.x

Zubkov, M., R. Holland, P. Burkhill, I. Croudace, and P. Warwick. 2007. Microbial abundance, activity and iron uptake in vicinity of the Crozet Isles in November 2004–January 2005. Deep-Sea Res. II **54:** 2126–2137, doi:10.1016/j.dsr2.2007.06.020

Associate editor: Mikhail V. Zubkov

Received: 31 January 2011
Amended: 30 August 2011
Accepted: 02 September 2011